Synthesis of Electrophiles Derived from Dimeric Aminoboranes and Assessing Their Utility in the Borylation of Nucleophiles

ORGANOMETALLICS

pubs.acs.org/Organometallics

Article

Synthesis of Electrophiles Derived from Dimeric Aminoboranes and Assessing Their Utility in the Borylation of π Nucleophiles

Clément R. P. Millet, Jürgen Pahl, Emily Noone, Kang Yuan, Gary S. Nichol, Marina Uzelac, and Michael J. Ingleson*

Cite This: https://doi.org/10.1021/acs.organomet.2c00393

Read Online

ACCESS | Metrics & More | Article Recommendations | Supporting Information

ABSTRACT: Dimeric aminoboranes, $[H_2BNR_2]_2$ (R = Me or CH_2CH_2) containing B_2N_2 cores, can be activated by I_2, $HNTf_2$ (NTf_2 = $[N(SO_2CF_3)_2]$), or $[Ph_3C][B(C_6F_5)_4]$ to form isolable $H_2B(\mu\text{-}NR_2)_2BHX$ (for X = I or NTf_2). For X = $[B(C_6F_5)_4]^-$ further reactivity, presumably between $[H_2B(\mu\text{-}NMe_2)_2BH][B(C_6F_5)_4]$ and aminoborane, forms a B_3N_3-based monocation containing a three-center two electron B-(μ-H)-B moiety. The structures of $H_2B(\mu\text{-}NMe_2)_2BH(I)$ and $[(\mu\text{-}NMe_2)BH(NTf_2)]_2$ indicated a sterically crowded environment around boron, and this leads to the less common O-bound mode of NTf_2 binding. While the iodide congener reacted very slowly with alkynes, the NTf_2 analogues were more reactive, with hydroboration of internal alkynes forming $(vinyl)_2BNR_2$ species and $R_2NBH(NTf_2)$ as the major products. Further studies indicated that the B_2N_2 core is maintained during the first hydroboration, and that it is during subsequent steps that B_2N_2 dissociation occurs. In the mono-boron systems, for example, $^iPr_2NBH(NTf_2)$, NTf_2 is N-bound; thus, they have less steric crowding around boron relative to the B_2N_2 systems. Notably, the monoboron systems are much less reactive in alkyne hydroboration than the B_2N_2-based bis-boranes, despite the former being three coordinate at boron while the latter are four coordinate at boron. Finally, these B_2N_2 electrophiles are much more prone to dissociate into mono-borane species than pyrazabole $[H_2B(\mu\text{-}N_2C_3H_3)]_2$ analogues, making them less useful for the directed diborylation of a single substrate.

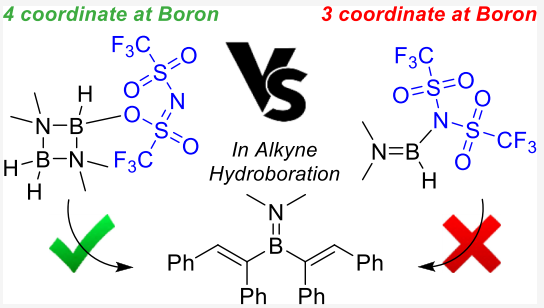

1. INTRODUCTION

Diboron compounds are of significant importance in synthesis, particularly through the use of tetra-alkoxydiboron(4)s, such as B_2Pin_2 (Figure 1, top), in transition-metal-catalyzed borylation reactions.[1] Recent years have seen a resurgence in the chemistry of more (relative to B_2Pin_2) electrophilic diboron(4) compounds. This has expanded on the work of Schlesinger using B_2X_4 (X = halide),[2] and a number of electrophilic diboron(4) compounds now have been reported, including examples that can borylate π nucleophiles and activate small molecules (e.g., H_2 and CO).[3] Parallel to this, there has been significant research into the chemistry of bidentate Lewis acids containing two electrophilic boron centers but no B−B bond, herein termed bis-boranes. While bis-boranes have been widely applied for small-molecule activation [e.g., in frustrated Lewis pairs (FLPs)][4] and in anion sensing,[5] the use of bis-boranes in the double borylation of π nucleophiles is relatively underexplored (*vide infra*).[6] This is despite the tunable nature of bis-boranes, particularly tailoring the B···B separation to match a specific substrate.

One of the most utilized classes of bis-boranes are 1,2-$C_6H_4(BX_2)_2$ (X = Cl or Br) and derivatives (e.g., 9,10-diboraanthracenes). While various groups demonstrated that these bis-borane ditopic Lewis acids can be used for small-molecule activation[7] and anion binding,[5] Wagner et al. demonstrated that they can be used for double electrophilic C−H borylation.[8] Specifically, compound **A** effected the double vicinal electrophilic C−H borylation of a range of aromatics to form B_2-doped polycyclic aromatic hydrocarbons (e.g., **B**). We recently extended this approach using bis-borane Lewis acids based on pyrazaboles (e.g., **C**),[9] which enabled the borylation-directed borylation of indoles and indolines (Figure 1, middle). Notably, the pyrazabole B_2N_4 core in **C** is sufficiently robust to persist during both electrophilic borylation steps (N−H and C−H), but it is reactive enough that it can be transformed subsequently into synthetically ubiquitous pinacol boronate esters. The B···B separation in **A** and **C** is ca. 3 Å, which is ideal for the vicinal functionalization of aromatics and the N/C7 functionalization of indoles. However, bis-borane Lewis acids with smaller B···B separations will be required for other substrates, for example, for accessing peri diborylated naphthalenes or 1,1-diborylated alkenes [where B···B separations in the double borylation products

Received: August 2, 2022

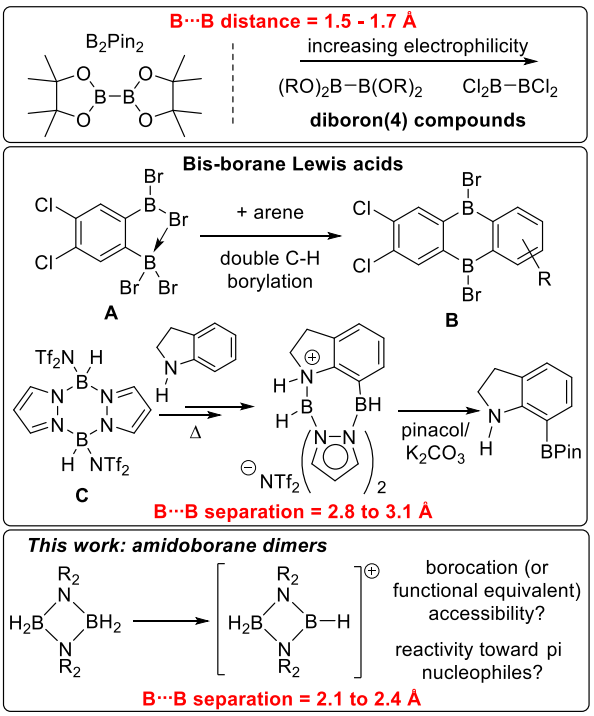

Figure 1. Top, diboron(4) compounds. Middle, bis-boranes able to effect double E–H borylation (E = N or C). Bottom, this work exploring electrophiles derived from dimeric aminoboranes.

containing a B-(μ-NMe_2)-B unit will be ca. 2.1–2.5 Å].[10,11] Thus, we were interested in accessing electrophiles derived from aminoborane dimers, $(H_2BNR_2)_2$, which have appropriate B···B separations and are simple to access. Herein, we report the synthesis, characterization, and reactivity studies toward π nucleophiles of a series of boron electrophiles derived from aminoborane dimers.

2. RESULTS AND DISCUSSION

Aminoboranes, R_2NBH_2, often exist in an equilibrium between dimeric and monomeric forms.[12] As a consequence of this sterically driven equilibrium, only a small number of aminoboranes are accessible as stable dimers in solution. Aminoboranes $[Me_2NBH_2]_2$, **1**, and $[(pyrrolidine)BH_2]_2$, **2**, were selected due to their inexpensive starting materials (Me_2NH/pyrrolidine and L-BH_3) and their dimeric form dominating in solution at room temperature (and even on heating). Importantly, solid state data for **1** and **2** show that they exhibit B···B separations of ca. 2.20 Å, which is in the desired region.[13] Furthermore, calculations on the hydride ion affinity (HIA) of a borenium cation derived from **1**,[14] $[\mathbf{D}]^+$, reveal it to have a high HIA. Indeed, the HIA of $[\mathbf{D}]^+$ is comparable to some of the most reactive (in electrophilic C–H borylation)[15] mono-boron cationic species (e.g., $[\mathbf{E}]^+$, Figure 2, inset) and greater than the HIA for borocations derived from pyrazabole.[9] Presumably, the high HIA for $[\mathbf{D}]^+$ is due to the absence of any π donors bound to boron and indicates that if borenium cations (or functional borenium equivalents)[14] can be accessed from **1** or **2**, they will be highly reactive species.

2.1. Synthesis of Electrophilic "B_2N_2" Aminoboranes.

Aminoboranes **1** and **2** were synthesized via catalyzed dehydrocoupling of the parent amine-borane following a reported method with lithium 2-^{t}Bu-pyridine.[16] A series of

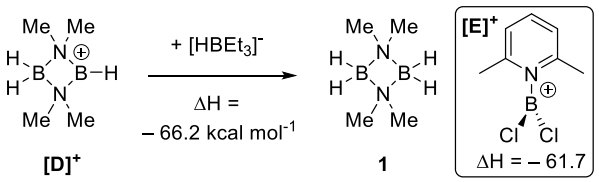

Figure 2. HIA calculations (relative to BEt_3) at M06-2x/6-311G(d,p)//PCM(DCM) (all calculations herein are performed at this level).

boron electrophiles derived from these precursors were targeted next. First **1** was treated with 0.5 equiv iodine (Figure 3, top), resulting in immediate hydrogen evolution and

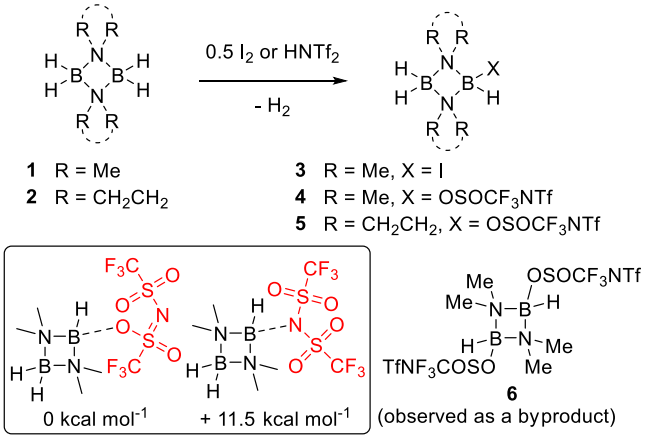

Figure 3. Top, the synthesis of compounds **3**–**5**. Inset bottom, the relative energies (ΔG) of O- and N-bound NTf_2 isomers of **4**. Bottom right, compound **6**, only isolated in our hands as a byproduct from the reaction between alkynes and **4** (*vide infra*).

formation of $H_2B(\mu\text{-}Me_2N)_2BH(I)$, **3**. Compound **3** was isolated by sublimation as a crystalline solid in 34% yield (though *in situ* conversion to **3** is effectively quantitative). The ^{11}B NMR spectrum of **3** revealed two distinct boron signals at δ_{11B} 3.9 (t, $^1J_{BH}$ = 118 Hz, BH_2) and 0.4 (d, $^1J_{BH}$ = 142 Hz, *B*HI), in accordance with the two different boron environments and their respective mono- and di-hydride substitution. The three inequivalent hydrides on the two boron centers were also observed by ^1H NMR spectroscopy (see Figure S10). X-ray diffraction (XRD) analysis confirmed the structure of **3** (*vide infra*), while IR spectroscopy confirmed only terminal B–H units. Notably, attempts to access a bis iodide derivative, $[Me_2NBH(I)]_2$, by adding excess iodine to **1** failed even after 3 days at room temperature. While heating did lead to slow further reactivity of **3** with I_2, this led to complex mixtures which contained monomeric species, for example, (amine)BI_3.

Mono and bis-borane systems, involving boron hydrides in combination with $HNTf_2$ (NTf_2 = $N(S(O)_2CF_3)_2$), have been used to generate reactive boron electrophiles[17] including examples which can effect C–B formation.[9,18] Thus, aminoboranes **1** and **2** were treated with one equivalent of $HNTf_2$ (Figure 3, top). Hydrogen evolution was observed, and $H_2B(\mu\text{-}Me_2N)_2BH(OSOCF_3NTf)$, **4**, and $H_2B(\mu\text{-pyrrolidine})_2BH(OSOCF_3NTf)$, **5**, were isolated in good yields (83 and 65%, respectively). The ^{11}B NMR spectrum of **4** displayed two signals at δ_{11B} 4.9 (d, $^1J_{BH}$ = 142 Hz, (H)*B*OSOCF$_3$NTf) and 3.3 (t, $^1J_{BH}$ = 119 Hz, BH_2). The ^{11}B NMR signals of **5** were overlapped, giving a multiplet (δ_{11B} 5.4–1.1), that turned into

https://doi.org/10.1021/acs.organomet.2c00393
Organometallics XXXX, XXX, XXX–XXX

two singlets in the $^{11}B\{^{1}H\}$ NMR spectrum (δ_{11B} 3.5 and 2.8) (see Figures S22 and S23). The ^{19}F NMR spectra of both **4** and **5** showed two fluorine resonances (**4** δ_{19F} = −75.7 and −78.5; **5** δ_{19F} = −75.7 and −78.4), indicating inequivalent CF_3 groups in the NTf_2 moiety. Similar ^{19}F NMR spectra have been reported by Vedejs and co-workers for $R_3N{-}BH_2NTf_2$ compounds where two fluorine resonances for B-NTf_2 corresponded to the O-bound NTf_2 isomer, in contrast to the more commonly found N-bound.[19] The mode of NTf_2 binding to boron is linked closely to the steric environment around boron, for example, $Me_3N{-}BH_2NTf_2$ has predominantly N-bound NTf_2 (7:1 N/O bound), while with $^{i}Pr_2NEt{-}BH_2NTf_2$, which contains a much larger amine, it is almost exclusively O-bound NTf_2. The existence of only O-bound NTf_2 in **4** and **5** suggests a relatively sterically encumbered boron center due to the four flanking methyl/CH_2 units. The complete absence (by ^{19}F NMR spectroscopy) of any N-bound isomer is also consistent with calculations which determined that the N-bound isomer of **4** to be 11.5 kcal mol^{-1} higher in energy than the O-bound isomer (Figure 3, inset). While multiple crystallization attempts for both **4** and **5** were unsuccessful, all data are consistent with NTf_2 being O-bound in both **4** and **5**, and IR spectroscopy was consistent with the presence of only terminal B−H units.

In an attempt to access a bis-NTf_2 analogue, $[(\mu\text{-}Me_2N)\text{-}BH(OSOCF_3NTf)]_2$, **6** (Figure 3, bottom right), compound **1** reacted with two equivalents of $HNTf_2$. While this led to rapid formation of **4**, further reactivity was only observed on heating. This led to slow consumption of **4** to form a complex mixture; notably, this contained mono-boron species (e.g., δ_{11B} = 27.1, d, $^{1}J_{BH}$ = 170 Hz—see Figure S80). It was not possible to isolate pure doubly activated diboron aminoboranes from these reactions for use in synthetic studies. However, it should be noted that **6** is accessible as it was isolated in very low quantity by fractional crystallization during reactivity studies between alkynes and **4** (*vide infra*) and was crystallographically characterized (*vide infra* for discussion).

Desirous of synthesizing a bis-borane aminoborane electrophile that exists as a separated ion pair with a planar three coordinate borocation, **1** was treated with one equivalent of $[Ph_3C][B(C_6F_5)_4]$ (Figure 4). The major product from this reaction, **7**, could be isolated by crystallization from layering a chlorobenzene solution with hexane. XRD analysis revealed the unexpected formation of the triboron monocation **7** (Figure 4, *vide infra* for structural discussion). The solid-state structure showed the formation of a salt, with a $[B(C_6F_5)_4]^-$ counter anion, but it was not the desired cation $[\mathbf{D}]^+$. Instead, the dimeric aminoborane **1** converted into a triboron species, containing a three-center two-electron B−H−B unit. The difference observed between forming **7** (with $[B(C_6F_5)_4]^-$) and **3**−**5** (with I^- or $[NTf_2]^-$) is attributed to the very weakly coordinating nature of $[B(C_6F_5)_4]^-$, which provides insufficient stabilization of the borocation $[\mathbf{D}]^+$.[20] Therefore, post hydride abstraction by Ph_3C^+, borocation $[\mathbf{D}]^+$ reacts further, presumably with remaining **1** through formal transfer of one Me_2NBH_2 unit from **1** to $[\mathbf{D}]^+$. The additional Me_2NBH_2 formally inserts into the N−BH^+ bond of $[\mathbf{D}]^+$, ultimately affording **7**. With the composition of **7** determined, modification of the stoichiometry to 3 equiv **1**:2 equiv $[Ph_3C][B(C_6F_5)_4]$ enabled **7** to be formed cleanly (by *in situ* NMR spectroscopy) and isolated in 70% yield.

Analysis of **7** by 2D and low-temperature NMR experiments enabled assignment of the ^{1}H and ^{13}C signals, which were in

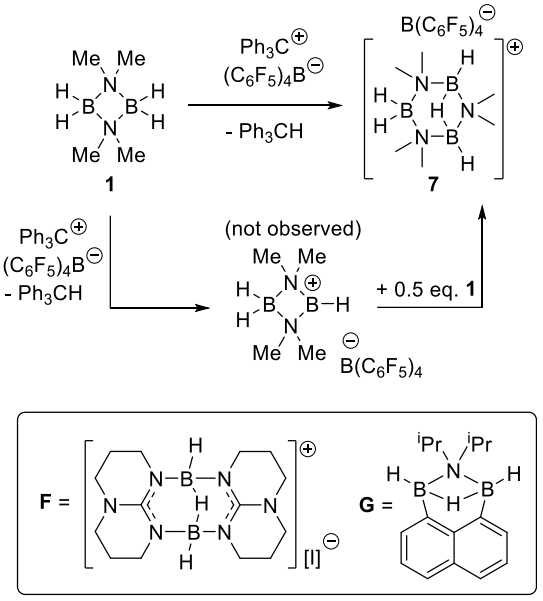

Figure 4. Top, synthesis of the cation **7**. Inset bottom, reported compounds with a comparable H−B(μ−H)B−H unit.

accordance with the solid-state structure, with the presence of the three different hydride environments confirmed by 2D $^{11}B{-}^{1}H$ HMQC (see Figure S33). The bridging hydride was significantly more shielded compared to the other hydrides in **7**, coming as a broad multiplet at δ 1.72−1.10 (vs 3.45−2.14 and 2.83−1.74 for the terminal hydrides). This chemical shift is in a similar region to that for the bridging hydride in the cation **F** reported by Himmel and co-workers (δ_{1H} 1.97, in C_6D_6).[21] Notably, the ^{11}B NMR spectrum of **7** showed a triplet (δ_{11B} 3.4, $^{1}J_{BH}$ = 120 Hz, BH_2) and a doublet (δ_{11B} −6.1, $^{1}J_{BH}$ = 164 Hz, H*B*(H)*B*H), with no coupling between the bridging hydride and the boron atoms observed. The absence of observable coupling with the bridging hydride in the ^{11}B NMR spectrum is consistent with related literature examples (e.g., **F** and **G**—Figure 4, inset bottom)[11,21] and is partly due to the smaller magnitude of $^{1}J_{B-H}$ coupling involving bridging hydrides (as reported in these related systems). While the additional B−H coupling was observed in higher-temperature NMR experiments for **G**, coupling with the bridging hydride was not observed at higher temperature for **7**, with decomposition of **7** occuring at higher temperatures.

Finally, to enable comparisons during reactivity studies, a strong electrophile derived from a monomeric aminoborane was targeted. Therefore, the more sterically encumbered aminoborane $(^{i}Pr)_2NBH_2$ (which exists as a monomer at room temperature) was reacted with $HNTf_2$ (Scheme 1). This reaction resulted in the immediate formation of the aminoborane adduct **8** instead of the desired product **9**, as evidenced by a boron resonance at δ_{11B} −9.5 (br, t, $^{1}J_{BH}$ = 123 Hz) and

Scheme 1. Synthesis of Electrophiles by Addition of $HNTf_2$ to a Monomeric Aminoborane

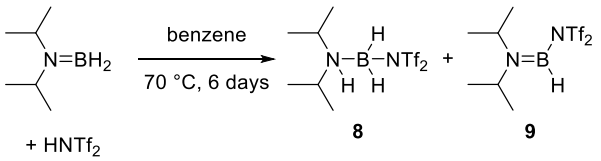

https://doi.org/10.1021/acs.organomet.2c00393
Organometallics XXXX, XXX, XXX−XXX

was confirmed further by ^{1}H, ^{13}C, and ^{19}F NMR spectroscopies (see Figures S40−S45). Heating **8** in benzene resulted in very slow conversion to **9**, which showed a signal in the ^{11}B NMR spectrum at δ 28.9 (d, $^{1}J_{BH}$ = 170 Hz); however, even after 7 days heating, a significant amount of **8** (ca. 60%) persisted. Therefore, compound **9** was isolated by fractional crystallization and characterized by ^{1}H, ^{13}C, and ^{19}F NMR spectroscopies. The single signal in the ^{19}F NMR spectrum (δ −73.2) indicated an N-bound triflimide, which was later confirmed by XRD analysis (*vide infra* for discussion). The switch from O-bound NTf_2 in the bis-borane structures of **4** and **5** to N-bound NTf_2 in **9** is notable and demonstrates the steric crowding present in dimeric aminoborane derivatives. Finally, it should be noted that resonances very close to the δ_{11B} of **8** (−6.5, t) and **9** (27.1, d) are observed in the reaction of **4** with $HNTf_2$, supporting the conclusion that monomeric boranes are being produced from combinations of **4** and two equiv $HNTf_2$.

2.2. Solid-State Structures. Crystals of **3** were obtained by sublimation and confirmed the formulation from NMR spectroscopy (Figure 5, left). The B···B distance in **3** (2.142(5) Å) is slightly shorter compared to its precursor **1**. Contrary to **1** that exhibits a planar N_2B_2 four-membered ring (Σ (internal angles of the N_2B_2 ring) = 360°), the unsymmetric substitution in **3** has distorted the N_2B_2 ring slightly into a butterfly conformation with the Σ (internal angles of the N_2B_2 ring) = 355°. A similar minor distortion was observed for an unsymmetric analogue, $Br_2B(\mu\text{-}Me_2N)_2BBr(OEt)$ (Σ (internal angle of the N_2B_2 ring) = 357°).[22] The larger iodine atom also causes other distortions in **3**, as evidenced by the large B2−B1−I1 angle of 142.9(2)°, a value greater than those in related substituted B_2N_2 compounds (where angles span the range 128−139°).[22,23] Furthermore, the incorporation of the less coordinating iodine leads to a shortening of the B1−N1 bond length (1.579(3) Å) and elongation of the B2−N1 bond length (1.614(4) Å), compared with its precursor **1**, where all the B−N bond lengths are 1.595−1.597 Å. The boron atom substituted with iodine shows a distorted tetrahedral geometry with a B−I bond of 2.252(4) Å, a slightly shorter distance compared with the B−I bond lengths reported for closely related compounds L-BH_2I (2.30−2.34 Å, L = N-heterocyclic carbenes or PR_3).[24]

The bis-NTf_2 derivative, $[(\mu\text{-}Me_2N)BH(OSOCF_3NTf)]_2$, **6** (Figure 5, right) was obtained as a byproduct from reactions between **4** and alkynes by fractional crystallization. Its solid-state structure revealed doubly O-bound triflimide moieties, which is in accordance with the O- versus N-bound equilibrium being sterically driven and the expected steric encumbrance around the core N_2B_2 ring (based on NMR data for **4**). **6** crystallizes as the trans isomer, which exhibits a large B1−O1−S1 angle (123.3(4)°) and a B1−O1 bond length of 1.526(7) Å, which is the shortest reported distance for an NTf_2 O bound to four coordinate boron.[17c,25] Note, the calculated B−O distance in **4** is comparable at 1.522 Å. Finally, the B···B distance in **6** (2.274(2) Å) is larger compared to **1** and **3**, possibly due to steric effects from the two NTf_2 units. While the four-membered ring of **6** is planar (Σ(internal angles) = 360°), the O-bound triflimides are impacting the core N_2B_2 ring with a noticeable difference observed between the B1−N1 bond lengths [1.589(8) and 1.662(10) Å], a difference larger than that in compound **3**.

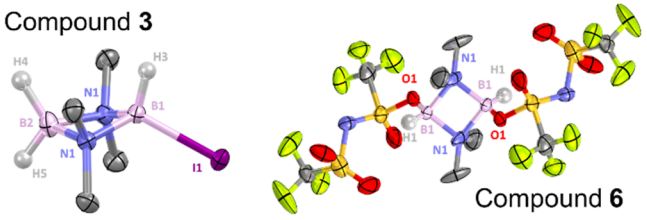

Figure 5. Left, the solid-state structure of **3** (50% ellipsoid probability). Hydrogen atoms except H3, H4, and H5 are omitted for clarity. Selected metrics [Å or °] for **3**: B···B = 2.142(5), B1−N1 = 1.579(3), B2−N1 = 1.614(4), B1−I1 = 2.252(4), and B2−B1−I1 = 142.9(2). Right, the solid-state structure of **6** (30% ellipsoid probability). Hydrogen atoms except H1 and disorder are omitted for clarity. Selected metrics [Å or °] for **6**: B···B = 2.274(2), B1−N1 = 1.589(8), B1−N1 = 1.662(10), B1−O1 = 1.526(7), B1−O1−S1 = 123.3(4), and B1−B1−O1 = 111.8(4).

To assess why N-binding of NTf_2 to the B_2N_2 cores in **4** is significantly higher in energy, the calculated structure of the non-observed N-bound isomer of **4**, **4-N**, was analyzed. The B−NMe_2 bonds (1.575 and 1.586 Å) are typical for boron-nitrogen single bonds at tetra-coordinate boron centers; however, the B−NTf_2 (1.626 Å) bond length is longer than the B-NTf_2 distance in a NTf_2 derivative of pyrazabole [1.609(2) Å] and a Ar_3P−BH(R)NTf_2 species,[17b] suggesting a weaker interaction in **4-N**. The N_2B_2 four-membered ring of **4-N** is found in a butterfly conformation and is more distorted than that in the case of **3**, with a Σ (internal angles of the N_2B_2 ring) = 351° (vs 355° in **3**). Most notably, a very large B−B-NTf_2 angle of 149.8° is found for **4-N**, much larger than the B1−B1−O1 angle observed in compound **6** (111.8(4)°) and even higher than that the B2−B1−I1 for **3** (142.9(2)°). These data highlight the steric effects that N-binding of NTf_2 to B_2N_2 cores imparts which is the likely reason why O-bound NTf_2 is observed experimentally in **4**−**6**.

Comparison of the calculated structure of **4-N** with the solid-state structure of the **9** is also informative as **9** also contains an N-bound NTf_2 (Figure 6, left). This is in accordance with a less hindered tricoordinate boron center. Notably, in **9**, the B1−NTf_2 exhibits a bond length of 1.586(15) Å, which is much shorter than that calculated for **4-N**, further indicating the significant steric crowding around the

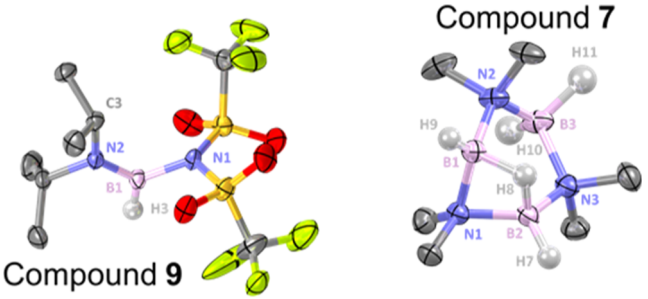

Figure 6. Left, the solid-state structure of **9** (50% ellipsoid probability). Hydrogen atoms except H3 are omitted for clarity. Selected metrics (Å or °) for **9**: B1−N1 = 1.566(4), B1−N2 = 1.370(4), and C3−N2−B1−N1 = −2.5(4). Right, the solid-state structure of **7** (50% ellipsoid probability). Hydrogen atoms except H7, H8, H9, H10, and H11 and the anion are omitted for clarity. Selected metrics (Å) for **7**: B1−N1 = 1.546(3), B1−N2 = 1.544(3), B2−N1 = 1.545(3), B2−N3 = 1.545(3), B3−N3 = 1.617(3), and B3−N2 = 1.617(3).

https://doi.org/10.1021/acs.organomet.2c00393
Organometallics XXXX, XXX, XXX−XXX

B_2N_2 cores. Furthermore, in **9**, a short B1−N2 bond length (1.351(17) Å) is observed, which is in the range of B═N double bonds (1.3−1.4 Å),[26] but it is shorter than previously reported $R_2N{=}BH_2$ species (e.g., 1.380(2) Å),[27] possibly due to enhanced electrophilicity at boron on substitution of H for NTf_2. The presence of a B═N unit in **9** is also confirmed by the very small C3−N2−B1−N1 torsion angle of −2.5(4)°.

Finally, the solid-state structure of **7** (Figure 6, right for the cationic component) represents a salt derived from the trimer $(BH_2)_3(NMe_2)_3$.[28] Contrary to neutral $(BH_2)_3(NMe_2)_3$, which exhibits a chair conformation, the cationic portion of **7** has a distorted boat conformation, with a planar B1−B2−N3−N2 central part [Σ (angle of N_2B_2) = 360°] and N1 and B3 orientated on the same face. The boron atoms B1 and B2, involved in the three-center two-electron B−H−B unit, exhibit shorter B−N bond lengths [between 1.544(3) and 1.546(3) Å) than B3 (1.617(3) Å], consistent with B1 and B2 being more electron-deficient boron centers. This is also indicated by the N−B bonds in neutral **G** being considerably longer [1.614(6) Å]. The B1···B2 distance at 1.912(4) in **7** is also shorter than that in **G** [1.971(7) Å]; this difference is not due to the peri substitution in **G** as the B···B separation in $(BBN)_2(\mu\text{-H})(\mu\text{-NMe}_2)$ is 1.975(4) Å. However, 1.912(4) Å is still longer than a B−B single bond, and we attribute this short B···B separation to the contracted N1−B bonds involving the bridging NMe_2 that are short as a result of the electron deficiency at B1 and B2 afforded by the cationic charge.

2.3. Reactivity Studies. With a series of bis-borane borocation equivalents isolated, we investigated briefly their reactivity toward simple bases. The significant steric crowding in **4** (indicated by the less common O-bound mode of NTf_2 coordination) was confirmed by the fact that **4** does not bind bulky Lewis bases such as P^tBu_3, or even PPh_3, in contrast to other reactive (but less hindered) borocations.[14] However, small nucleophilic bases do react with these bis-borane electrophiles, but they lead to cleavage of the B_2N_2 core. For example, the addition of 4-DMAP to **4** led to the precipitation of a solid that was confirmed by X-ray crystallographic studies to be the mono-boron species $[(4\text{-DMAP})_2BH_2][NTf_2]$ (see Figure S82).

Moving to π nucleophiles, reactions between **3** and naphthalene, N−H-indole, N−Me-indole, or *N*-methylaniline gave no evidence for C−H borylation at ambient and raised temperatures, although indole hydroboration was observed. Similarly, no C−H borylation was observed for reactions between **4** and N−H-indole, N−Me-indole, or *N*-methylaniline (with or without 2,6-di-*tert*-butyl-4-methylpyridine as an exogenous base). As reduction of indoles to indolines is a known reaction achievable with L-BH_3,[29] these reactions were not investigated further. We turned our attention next to alkene and alkyne functionalization. When stilbene was combined with **3**, this gave no reaction. Hydroboration of stilbene by **4** was observed by ^{1}H NMR spectroscopy; however, the slow rate of the reaction coupled with the formation of multiple species meant we did not pursue this reaction. Terminal alkynes treated with **4** reacted in a faster manner but led to the complex intractable mixtures; however, the reactivity with internal alkynes was cleaner. Reacting **4** with diphenylacetylene led to two new signals in the ^{11}B NMR spectrum at δ_{11B} 40.0 (br, s) and 27.7 (d, $^1J_{BH}$ = 180 Hz), while ^{1}H NMR spectroscopy indicated the formation of a single hydroboration product (a vinylic C−H was observed at δ_{1H} 6.75 ppm). While the reaction is slow at 70 °C, higher temperatures cannot be used due to the limited stability of **4** in solution at raised temperatures. The δ_{11B} = 40 product was also observed using **3**, but this reaction was extremely slow (≈5% internal conversion vs an internal standard, after 5 days heating), consistent with the stronger coordination of iodide to boron relative to triflimide. Therefore, only reactivity with NTf_2 derivatives is discussed from hereon. The broad signal at δ_{11B} = 40.0 is consistent with the formation of an $R_2B{=}NMe_2$ species,[30] with R in this case presumably vinyl groups formed from the hydroboration of the alkyne to form **10** (Scheme 2).

Scheme 2. Hydroboration of Diphenylacetylene with 4[a]

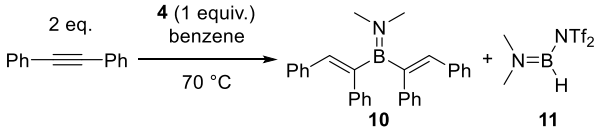

[a]Internal conversion (vs an internal standard) ≈ 95% (after 4.5 days).

Further NMR experiments allowed us to confirm the formation of the divinylaminoborane **10** (see Figures S56−S60). No change in the reaction outcome was observed on repeating in the presence of exogenous base (in an attempt to effect intramolecular aryl C−H borylation after the initial hydroboration).

Notably, the second observed signal at δ_{11B} = 27.7 while close to that reported for $(Me_2N)_2BH$ (δ_{11B} 26−29, $^1J_{BH}$ = 135−139 Hz),[31] exhibited a $^1J_{BH}$ = 180 Hz. This is more consistent with the formation of **11** (Scheme 2), which is closely comparable in spectroscopic data to **9**. The B_2N_2 core of **4** has split during formation of **10** and **11**, with **10** the product derived from the formal hydroboration of two equivalents of diphenylacetylene with $Me_2N{=}BH_2$, while **11** is then the expected byproduct to maintain mass balance. Stoichiometry studies confirmed the full consumption of all diphenylacetylene, and **4** occurs only at a ratio of 2:1. Crystallization of a reaction mixture post hydroboration enabled isolation (in a very small quantity) and structural characterization of the dimer of **11**, compound **6**. As discussed above **6** contains two O-bound NTf_2, whereas in the monomeric derivatives **11** and **9**, NTf_2 is N-bound (by ^{19}F NMR spectroscopy and by crystallographic analysis for **9**). A sufficient quantity of pure **6** for NMR analysis was not obtainable by fractional crystallization, precluding full analysis. Nevertheless, the observation of O-bound NTf_2 in the solid-state structure of **6** is consistent with the NMR data for **4** and calculations (the O-bound isomer of **4** is more stable than the N-bound by 11.5 kcal mol^{-1}), in contrast calculations on the isomers of **11** (**11-O** and **11**, respectively) show that the N-bound NTf_2 isomer is more stable by 1.6 kcal mol^{-1} than **11-O** (Figure 7, top inset), consistent with a less sterically encumbered boron center in **11** (relative to **4**).

The mechanism for the hydroboration of diphenylacetylene starting from **4** at raised temperature could proceed via bis-borane **4**, or via mono-boron species derived from the dissociation of **4** at raised temperatures. No significant hydroboration of diphenylacetylene was observed when it was treated with **1** or the mono-boron species $^i Pr_2NBH_2$ indicating the need for an electrophilic borane (Figure 7, bottom—see Figures S68−S75). More notably, $^i Pr_2NBH(NTf_2)$, **9**, also did not affect hydroboration (<5% after 4 days at 70 °C). This indicates the necessity of an electrophilic bis-

https://doi.org/10.1021/acs.organomet.2c00393
Organometallics XXXX, XXX, XXX−XXX

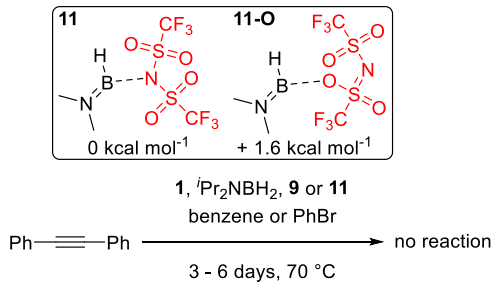

Figure 7. Inset, relative stability of **11** and **11-O**. Bottom, absence of reactivity from **1**, $^{i}Pr_2NBH_2$, and **9** toward diphenyl-acetylene.

borane (as in **4**) for hydroboration to occur in these aminoborane systems. This is supported by the observation of **11** at the end of the reactions starting from **4** (even when using excess diphenylacetylene), indicating that **11** also does not hydroborate diphenylacetylene under these conditions. Therefore, the hydroboration of the first equivalent of diphenylacetylene occurs via the bis-borane **4** and not via mono-borane species from the dissociation of **4**. No intermediates between **4** and **10** are observed by NMR spectroscopy; thus, the subsequent steps occur rapidly relative to the first step of the reaction. Decreasing the temperature and the polarity of the solvent slowed the reaction rate; however, the reaction was cleanest in benzene (relative to reactions in haloarenes), therefore only reactions in benzene are discussed.

The disparity in reactivity towards diphenylacetylene of **4** versus **9**/**11** is notable as it indicates that a four coordinate at boron B-NTf_2 species (in **4**) is more reactive in hydroboration than a three coordinate at boron B-NTf_2 species (in **9**/**11**). However, it should be noted that in the mono-boron $R_2N{=}BH(NTf_2)$ compounds there is significant $B{=}NR_2$ multiple bond character; thus, the reaction of **4** and **9**/**11** with alkynes are all expected to proceed via displacement of NTf_2 (by an S_N1 or an S_N2 at boron mechanism). Significant B=N character precluding hydroboration is supported by $^{i}Pr_2N{=}BH_2$, not effecting alkyne hydroboration under these conditions. If the hydroboration reaction with **4** or **9**/**11** proceeds via an S_N1-type mechanism, then this would require dissociation of NTf_2 from boron and formation of borenium (e.g., $[\mathbf{D}]^+$ from **4**) or borinium (e.g., $[R_2N{=}B{-}H]^+$ from **9**/**11**) cations. Borenium cations are much more energetically accessible than borinium cations, and we have recently shown that $[R_2N{=}BY]^+$ borinium cations are extremely high in energy and not feasible intermediates in C−H borylation.[32] If an S_N2-type mechanism is operative, the absence of any diphenylacetylene hydroboration starting from **9**/**11** can be attributed to the stronger binding of NTf_2 to boron via nitrogen relative to O-bound NTf_2 (as found in bis-borane **4**), leading to a higher reaction barrier.

With a better understanding of the reaction, the regioselectivity in the hydroboration of an unsymmetric alkyne was probed. Hydroboration of 1-phenyl-1-propyne afforded a mixture of isomers, **12a**, **12b**, and **12c** (Scheme 3), in a ratio of 29:54:17 (see Figure S63) in a conversion of 81%. The Markovnikov/anti-Markovnikov regioselectivity therefore is low using **4** and is comparable to that previously reported for the hydroboration of the same substrate with (2,6-lutidine)BH_2I.[18] Attempts to alter the regioselectivity by varying the reaction conditions did not lead to any significant improvement. Furthermore, the use of **5** also led to a mixture

Scheme 3. Synthesis of 12a−c[a]

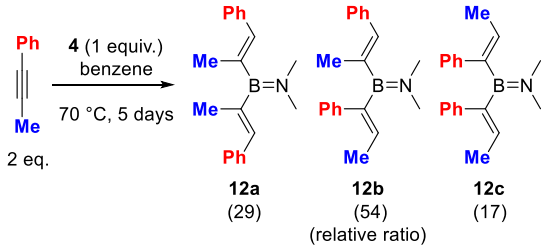

[a]Internal conversion (vs an internal standard) ≈ 81% (after 5 days).

of hydroboration isomers but the complexity of the *in situ* ^{1}H NMR spectra (on switching NMe_2 for pyrrolidine) precluded determination of the exact ratios in this case. It should be noted that while **10** and **12** proved unstable to silica gel or distillation, fractional crystallization from pentane at low temperature afforded sufficiently pure material to enable the full characterization (see Figures S56−60 and S64−66).

Finally, we were interested in understanding the greater propensity of these dimeric aminoborane derivatives to cleave to form mono-boron species compared to pyrazabole derivatives as the dissociation of **3** and **4** into mono-boron species is undesirable for their use in borylation-directed borylation.[9] It was found that the dissociation was much more endergonic in the case of pyrazabole than that for $[Me_2NBH_2]_2$, **1** (Scheme 4). This is in accordance with the

Scheme 4. Comparison of the Energy Change during Dissociation of Pyrazabole, 1, and 4 into Their Respective Mono-Boron Species

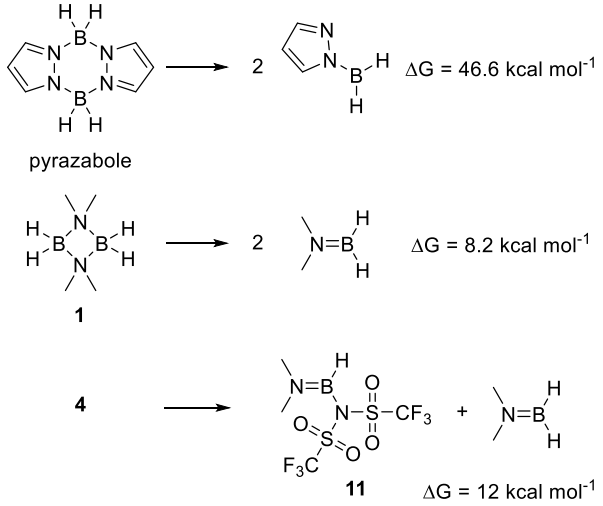

lower stability observed in reactivity studies with the bis-borane aminoborane systems (e.g., **3** and **4**) relative to the pyrazaboles. We attribute this in part to ring strain in dimeric aminoboranes and the greater π donor ability of a NMe_2 group relative to a pyrazole unit (where the N lone pair is part of the aromatic system) that helps stabilize the BH_2 center in the monomeric form.

It should also be noted that substitution of H for NTf_2 only alters the energy involved in dissociation of the bis-borane by a small amount ($\delta\Delta G$ = 3.8 kcal mol^{-1}, Scheme 4 bottom); thus, it can also can be expected to split into mono-boron species to some degree, particularly on heating. Notably, heating **4** for 3 days in benzene at 100 °C (in a sealed tube) led to the

https://doi.org/10.1021/acs.organomet.2c00393
Organometallics XXXX, XXX, XXX−XXX

observation (by ^{11}B NMR spectroscopy) of small quantities of **11**. The fact that **11** is observed at room temperature from this reaction, that is, it is not consumed to reform **4** on cooling, was surprising based on the DFT calculations. This observation is attributed tentatively to a significant kinetic barrier associated with the linkage isomerism that has to occur to convert from N-bound NTf_2 in **11** to form O-bound NTf_2 in **4**.

3. CONCLUSIONS

In conclusion, a series of dimeric aminoborane-derived electrophiles were synthesized using readily accessible starting material. The optimal coordinating ability of the anion X to boron in $H_2B(\mu\text{-}NR_2)_2BHX$ electrophiles is crucial, with iodide proving too coordinating (inhibiting reactivity with π nucleophiles), while $[B(C_6F_5)_4]^-$ is insufficiently coordinating which leads to further reactivity to form a B_3N_3-based cation. Triflimide (NTf_2) proved to be optimal, enabling bis-borane electrophiles with B_2N_2 cores to be accessed that do react relatively cleanly with certain π nucleophiles. Thus, hydroboration of internal alkynes was achieved using $H_2B(\mu\text{-}NR_2)_2BH(NTf_2)$ with the B_2N_2 core maintained during the first hydroboration but subsequently splitting to ultimately produce $R_2N{=}B(vinyl)_2$. Notably, mono-boron analogues, for example, $R_2NBH(NTf_2)$ exist with N-bound NTf_2 in contrast to the bis-boranes and are much less reactive in alkyne hydroboration. This represents an unusual case where the four coordinate at boron species, $H_2B(\mu\text{-}NR_2)_2BH(NTf_2)$, is more reactive than a three coordinate at boron analogue $R_2NBH(NTf_2)$. Finally, the stability of dimeric bis-boranes with respect to dissociation into monomers needs to be carefully considered for use in borylation-directed borylation, with the B_2N_2 core in dimeric aminoboranes too weakly bound for that particular application.

4. EXPERIMENTAL SECTION

4.1. General Materials and Methods. All reactions were performed under inert conditions using standard Schlenk techniques or in an MBraun Unilab glovebox (<0.1 ppm H_2O/O_2). Unless otherwise stated, solvents were degassed with nitrogen, dried over activated aluminum oxide (Solvent Purification System: Inert PureSolv MD5 SPS), and stored over 3 Å molecular sieves in ampules equipped with Young's valves. Chlorobenzene, 1,2-difluorobenzene, and 1,2-dichlorobenzene were dried over calcium hydride, distilled, and stored over 3 Å molecular sieves. Deuterated solvents [$CDCl_3$, C_6D_6, and C_6D_5Br (99.6% D, Sigma-Aldrich)] were dried and stored over 3 Å molecular sieves. All chemicals were, unless stated otherwise, purchased from commercial sources and used as received. $BH_3{\cdot}SMe_2$ was transferred to an ampule fitted with Young's valve prior to use. $[Ph_3C][B(C_6F_5)_4]$ and lithium 2-^{t}Bu-dihydropyridine were synthesized following the literature procedure.[33,34] NMR spectra [^{1}H, ^{1}H{^{11}B}, ^{11}B, ^{11}B{^{1}H}, ^{13}C{^{1}H}, and ^{19}F] were recorded on Bruker Avance III 400 MHz, Bruker Avance III 500 MHz, Bruker Avance III 600 MHz, or Bruker PRO 500 MHz spectrometers. Chemical shifts (δ) are quoted in parts per million (ppm), and coupling constants (J) are given in hertz (Hz) to the nearest 0.5 Hz and as positive values regardless of their real individual signs. ^{1}H and ^{13}C shifts are referenced to the appropriate residual solvent peak, while ^{11}B and ^{19}F shifts are referenced relative to external $BF_3{\cdot}Et_2O$ and C_6F_6, respectively. Abbreviations used are s (singlet), d (doublet), t (triplet), q (quartet), sep (septet), m (multiplet), and br (broad). Background signals in ^{11}B NMR spectra arise to a significant degree from glass components of the probes used in our spectrometers. Unless otherwise stated, all NMR spectra were recorded at 20 °C. Mass spectrometry was performed at the Scottish Instrumentation and Resource Centre for Advanced Mass Spectrometry (SIRCAMS) at the University of Edinburgh using electron impact (EI) or electrospray ionization (ESI) techniques. CHN elemental analyses were carried out by Elemental Microanalysis Ltd. FTIR spectra were recorded on Shimadzu IRAffinity-1S FTIR.

4.2. Synthesis of Boron Electrophiles and Precursors. *4.2.1. Preparation of $[Me_2NBH_2]_2$, **1**.* Borane dimethylamine complex (3.00 g, 51.00 mmol, 1.00 equiv) and lithium 2-^{t}Bu-dihydropyridine (0.18 g, 1.30 mmol, 2.5 mol %) were added to a Schlenk flask. Using a bend adapter tube, the flask was connected to a second Schlenk flask, immersed in an ice bath. The mixture was heated overnight at 100 °C with the collection Schlenk flask being left opened to the nitrogen atmosphere. The product started subliming during overnight heating. More product **1** was isolated by further sublimation (heat-gun under N_2) as colorless crystals in 55% yield (1.58 g, 13.92 mmol). Analytical data were in accordance with literature values.[35] ^{1}H NMR (500 MHz, $CDCl_3$, 300 K): δ 2.64 (1:1:1:1, q, $^1J_{HB}$ = 112 Hz, 4H, B*H*), 2.45 (s, 12H, N(CH_3)$_2$); ^{11}B NMR (160 MHz, $CDCl_3$, 300 K): δ 5.2 (t, $^1J_{BH}$ = 112 Hz, *B*H); ^{11}B {^{1}H} NMR (160 MHz, $CDCl_3$, 300 K): δ 5.2 (s, *B*H); ^{13}C {^{1}H} NMR (126 MHz, $CDCl_3$, 300 K): δ 51.93 (s, N(CH_3)$_2$).

*4.2.2. Preparation of [Pyrrolidine-BH_2]$_2$, **2**.* Neat $BH_3{\cdot}Me_2S$ (2.63 mL, 27.70 mmol, 1.00 equiv) was slowly added to a solution of pyrrolidine (2.00 g, 27.70 mmol, 1.00 equiv) in pentane (30 mL) at room temperature. The solution was stirred for 1 h. Volatiles were removed *in vacuo* affording the pyrrolidine·BH_3 adduct as a white solid. Lithium 2-^{t}Bu-dihydropyridine (0.10 g, 0.69 mmol, 2.5 mol %) was added to the crude pyrrolidine·BH_3 adduct, and the mixture was heated overnight at 100 °C in an unpressurized system. Product **2** was isolated by distillation (100 °C, 10^{-3} to 10^{-2} mbar) as a colorless waxy solid in 80% yield (1.84 g, 11.09 mmol). Analytical data were in accordance with literature values.[36] ^{1}H NMR (500 MHz, $CDCl_3$, 300 K): δ 2.86 (br, t, 8H, NCH_2CH$_2$), 2.61 (1:1:1:1, q, $^1J_{HB}$ = 112 Hz, 4H, B*H*), 1.76−1.66 (m, 8H, NCH$_2$CH_2); ^{11}B NMR (160 MHz, $CDCl_3$, 300 K): δ 3.0 (t, $^1J_{BH}$ = 112 Hz, *B*H); ^{11}B {^{1}H} NMR (160 MHz, $CDCl_3$, 300 K): δ 3.0 (s, *B*H); ^{13}C {^{1}H} NMR (126 MHz, $CDCl_3$, 300 K): δ 60.08 (s, NCH_2CH$_2$), 23.62 (s, NCH$_2$CH_2).

*4.2.3. Preparation of $H_2B(\mu\text{-}Me_2N)_2BH$(I), **3**.* Iodine (0.54 g, 2.11 mmol, 0.48 equiv) was dissolved in benzene (10 mL) and slowly added to a solution of $[Me_2NBH_2]_2$ (0.50 g, 4.39 mmol, 1.00 equiv) in benzene (10 mL) at room temperature. The resulting solution was stirred at room temperature for 30 min. The volatiles were removed under vacuum with care, to avoid the solid product subliming during the process. The product was extracted with pentane (5 mL). After vacuuming the volatiles, the product **3** was isolated by sublimation under vacuum (heat-gun, 10^{-3} to 10^{-2} mbar) as a colorless crystalline solid in 34% yield (0.35 g, 1.47 mmol). ^{1}H NMR (500 MHz, C_6D_6, 300 K): δ 4.37 (1:1:1:1, q, $^1J_{HB}$ = 142 Hz, 1H, B*H*I), 2.88 (1:1:1:1, q, $^1J_{HB}$ = 119 Hz, 1H, B*H*), 2.69 (1:1:1:1, q, $^1J_{HB}$ = 115 Hz, 1H, B*H*), 2.22 (s, 6H, (NCH_3)$_2$), 2.00 (s, 6H, (NCH_3)$_2$); ^{11}B NMR (160 MHz, C_6D_6, 300 K): δ 3.9 (t, $^1J_{BH}$ = 118 Hz, *B*H$_2$), 0.4 (d, $^1J_{BH}$ = 142 Hz, *B*HI); ^{11}B {^{1}H} NMR (160 MHz, C_6D_6, 300 K): δ 3.9 (s, *B*H$_2$), 0.4 (s, *B*HI); ^{13}C {^{1}H} NMR (126 MHz, C_6D_6, 300 K): δ 51.24 (s, (NCH$_3$)$_2$), 49.86 (s, (NCH$_3$)$_2$) (see Figure S1). Elemental analysis: calculated for $C_4H_{15}B_2N_2I$: C 20.04%, H 6.31%, N 11.69%; observed: C 20.67%, H 6.46%, N 11.53%. IR: (ν_{max} (neat)/cm^{-1}) 2499 (B−H), 2432 (B−H), 2358 (B−H).

*4.2.4. Preparation of $H_2B(\mu\text{-}Me_2N)_2BH(OSOCF_3NTf)$, **4**.* $HNTf_2$ (1.18 g, 4.18 mmol, 1.00 equiv) was dissolved in benzene (10 mL) and slowly added to a solution of $[Me_2NBH_2]_2$ (0.50 g, 4.39 mmol, 1.05 equiv) in benzene (10 mL) at room temperature. The solution was stirred at room temperature for 24 h. The volatiles were removed under vacuum. The product was extracted with pentane (10 mL). Drying under vacuum for 1 h afforded the product **4** as a colorless oil in 83% yield (1.37 g, 3.48 mmol). ^{1}H NMR (500 MHz, C_6D_6, 300 K): δ 3.14 (br, q, $^1J_{HB}$ = 138 Hz, 1H, B(*H*)OS(O)(CF$_3$)NTf), 2.33 (br, q, $^1J_{HB}$ = 123 Hz, 2H, B*H*$_2$), 1.96 (s, 3H, CH_3), 1.88 (s, 3H, CH_3), 1.87 (s, 3H, CH_3), 1.79 (s, 3H, CH_3); ^{1}H {^{11}B} NMR (500 MHz, C_6D_6, 300 K): δ 3.14 (br, s, 1H, B(*H*)OS(O)(CF$_3$)NTf), 2.33 (br, s, 2H, B*H*$_2$), 1.97 (s, 3H, CH_3), 1.88 (s, 3H, CH_3), 1.87 (s, 3H, CH_3), 1.80 (s, 3H, CH_3); ^{11}B NMR (160 MHz, C_6D_6, 300 K): δ 4.9 (d, $^1J_{BH}$ = 142 Hz, *B*(H)OS(O)(CF$_3$)NTf), 3.3 (t, $^1J_{BH}$ = 119 Hz,

https://doi.org/10.1021/acs.organomet.2c00393
Organometallics XXXX, XXX, XXX−XXX

BH_2); ^{11}B {^1H} NMR (160 MHz, C_6D_6, 300 K): δ 4.9 (s, B(H)OS(O)(CF_3)NTf), 3.3 (s, BH_2); ^{13}C {^1H} NMR (126 MHz, C_6D_6, 300 K): δ 119.99 (q, $^1J_{CF}$ = 320 Hz, CF_3), 119.43 (q, $^1J_{CF}$ = 321 Hz, CF_3), 49.40 (s, CH_3), 49.32 (s, CH_3), 44.48 (s, CH_3), 44.43 (s, CH_3); ^{19}F NMR (471 MHz, C_6D_6, 300 K): δ −75.7 (s, 3F, CF_3), −78.5 (s, 3F, CF_3). Elemental analysis: calculated for $C_6H_{15}B_2F_6N_3O_4S_2$: C 18.34%, H 3.85%, N 10.69%; observed: C 18.40%, H 3.62%, N 10.50%. IR: (ν_{max} (neat)/cm^{-1}) 2515 (B−H), 2474 (B−H), 2372 (B−H).

*4.2.5. Preparation of $H_2B(\mu$-pyrrolidine$)_2BH(OSOCF_3NTf)$, **5**.* $HNTf_2$ (1.21 g, 4.30 mmol, 1.00 equiv) was dissolved in benzene (10 mL) and slowly added to a solution of [pyrrolidine-BH_2]$_2$ (0.75 g, 4.52 mmol, 1.05 equiv) in benzene (10 mL) at room temperature. The solution was stirred at room temperature for 20 h. The volatiles were removed under vacuum. The product was extracted with pentane (10 mL). Drying under vacuum overnight at 40 °C afforded the product **5** as a colorless oil in 65% yield (1.24 g, 2.79 mmol). ^1H NMR (500 MHz, C_6D_6, 300 K): δ 4.00−2.90 (br, m, 1H, B(H)OS(O)(CF_3)NTf), 2.88−1.96 (m, 10H, NCH_2CH_2 and BH_2), 1.35−1.11 (m, 8H, NCH_2CH_2); ^1H {^{11}B} NMR (500 MHz, C_6D_6, 300 K): δ 3.43 (br, s, 1H, B(H)OS(O)(CF_3)NTf), 2.88−1.96 (m, 10H, NCH_2CH_2 and BH_2), 1.35−1.11 (m, 8H, NCH_2CH_2); ^{11}B NMR (160 MHz, C_6D_6, 300 K): δ 5.4−1.1 (m, B(H)OS(O)(CF_3)-NTf, BH_2); ^{11}B {^1H} NMR (160 MHz, C_6D_6, 300 K): δ 3.5 (s, B(H)OS(O)(CF_3)NTf), 2.8 (s, BH_2); ^{13}C {^1H} NMR (126 MHz, C_6D_6, 300 K): δ 120.05 (q, $^1J_{CF}$ = 320 Hz, CF_3), 119.49 (q, $^1J_{CF}$ = 322 Hz, CF_3), 58.62 (s, NCH_2CH_2), 58.55 (s, NCH_2CH_2), 53.85 (s, NCH_2CH_2), 22.89 (s, NCH_2CH_2), 22.88 (s, NCH_2CH_2), 22.79 (s, NCH_2CH_2), 22.78 (s, NCH_2CH_2); ^{19}F NMR (471 MHz, C_6D_6, 300 K): δ −75.7 (s, 3F, CF_3), −78.4 (s, 3F, CF_3). Elemental analysis: calculated for $C_{10}H_{19}B_2F_6N_3O_4S_2$: C 26.99%, H 4.30%, N 9.44%; observed: C 26.94%, H 4.18%, N 9.39%. IR: (ν_{max} (neat)/cm^{-1}) 2499 (B−H), 2451 (B−H), 2374 (B−H).

*4.2.6. Preparation of $[(Me_2N)_3B_3H_5][B(C_6F_5)_4]$, **7**.* $(Me_2NBH_2)_2$ (0.03 g, 0.22 mmol, 3.00 equiv) and $[Ph_3C][B(C_6F_5)_4]$ (0.14 g, 0.15 mmol, 2 equiv) were dissolved in PhCl (3 mL) and heated to 60 °C until the solution turned colorless (30 min). The solution was carefully layered with hexane (5 mL). After 21 days, the formed colorless crystals were washed with hexane (2 × 2 mL) and dried *in vacuo*. The product **7** was isolated as colorless crystals in 70% yield (0.09 g, 0.10 mmol). ^1H NMR[a,b] (500 MHz, $C_6H_4F_2$, 300 K): δ 3.45−2.14 (br, m, 2H, HB(H)BH), 3.45−1.74 (br, m, 18H, N(CH_3)$_2$), 2.83−1.74 (br, m, 2H, BH_2), 1.72−1.10 (br, m, 1H, HB(H)BH); ^1H NMR[a] (500 MHz, $C_6H_4F_2$, 278 K): δ 3.45−2.14 (br, m, 2H, HB(H)BH), 3.13 (s, 3H, N(CH_3)), 2.83−1.74 (br, m, 2H, BH_2), 2.55 (s, 6H, N(CH_3)), 2.47 (s, 6H, N(CH_3)), 2.36 (s, 3H, N(CH_3)), 1.72−1.10 (br, m, 1H, HB(H)BH); ^1H {^{11}B} NMR[a,b] (500 MHz, $C_6H_4F_2$, 300 K): δ 3.45−2.14 (br, m, 2H, HB(H)BH), 3.45−1.74 (br, m, 18H, N(CH_3)$_2$), 2.83−1.74 (br, m, 2H, BH_2), 1.52 (br, s, 1H, HB(H)BH); ^{11}B NMR[a] (160 MHz, $C_6H_4F_2$, 300 K): δ 3.4 (t, $^1J_{BH}$ = 120 Hz, BH_2), −6.1 (br, d, $^1J_{BH}$ = 164 Hz, HB(H)BH), −16.2 (s, $B(C_6F_5)_4$); ^{11}B {^1H} NMR[a] (160 MHz, $C_6H_4F_2$, 300 K): δ 3.4 (s, BH_2), −6.1 (s, HB(H)BH), −16.2 (s, $B(C_6F_5)_4$); ^{13}C {^1H} NMR[a] (126 MHz, $C_6H_4F_2$, 300 K): δ 148.8 (br, m, C_{ortho}F), 140.6 (br, t, C_{para}F), 138.6 (br, m, C_{meta}F), 136.7 (br, m, C_{ipso}F), 54.3 (br, s, N(CH_3)), 49.8 (br, s, N(CH_3)), 46.4 (br, s, N(CH_3)), 40.1 (br, s, N(CH_3)); ^{19}F NMR[a] (471 MHz, $C_6H_4F_2$, 300 K): δ −132.5 (br, s, CF_{ortho}), −163.9 (t, $^3J_{FF}$ = 20 Hz, CF_{para}), −167.7 (br, t, $^3J_{FF}$ = 17 Hz, CF_{meta}).[a] Due to solubility and stability issues, NMR data of **7** were recorded in 1,2-difluorobenzene ($C_6H_4F_2$). Reference NMR experiments using $SiMe_4$ were carried out to determine the ^1H and ^{13}C shifts of 1,2-difluorobenzene. Hydrogen atoms located on boron centers [BH_2, HB(H)BH, and HB(H)BH] were identified by the 2D ^{11}B−^1H HMQC experiment. Mass spectrum: HRMS (ESI+) m/z: calcd for $C_6H_{23}B_3N_3^+$: 170.21657; found: 170.21576. IR: (ν_{max} (neat)/cm^{-1}) 2538 (B−H), 2465 (B−H), 2403 (B−H).

*4.2.7. Preparation of **10**.* A solution of $H_2B(\mu$-$Me_2N)_2BH$-($OSOCF_3NTf$), **4** (0.22 g, 0.56 mmol, 1.00 equiv) in benzene (1 mL) was added to a solution of diphenylacetylene (0.20 g, 1.12 mmol, 2.00 equiv) in benzene (1 mL). The resulting solution was heated at 70 °C for 1 week. While heating, the solution turned slowly from colorless to dark orange. The volatiles were removed under vacuum, affording an oil. The oil was extracted with pentane (2 mL), giving a clear orange solution. The solution was cooled to −35 °C and filtered at this temperature. Removal of volatiles *in vacuo* afforded the product **10** as an orange oil (0.11 g), contaminated with remaining trace of $-NTf_2$ side-products. ^1H NMR (500 MHz, C_6D_6, 300 K): δ 7.23−7.19 (m, 4H), 7.15−7.12 (m, 4H), 7.12−7.08 (m, 4H), 7.03−6.99 (m, 2H), 6.99−6.94 (m, 4H), 6.92−6.88 (m, 2H), 6.75 (s, 2H), 2.68 (s, 6H); ^{11}B NMR (160 MHz, C_6D_6, 300 K): δ 40.0 (br, s, $BN(Me)_2$); ^{13}C {^1H} NMR (126 MHz, C_6D_6, 300 K): δ 147.43 (br), 142.95, 138.50, 134.72, 129.77, 129.03, 128.82, 128.27[a], 126.90, 126.29, 40.99. Mass spectrum: HRMS (ESI+) m/z: calcd for $C_{30}H_{28}BN$: 413.23093; found: 413.23142.

■ ASSOCIATED CONTENT

Supporting Information

The Supporting Information is available free of charge at https://pubs.acs.org/doi/10.1021/acs.organomet.2c00393.

NMR spectra (PDF)

Coordinates for calculated compounds (XYZ)

Accession Codes

CCDC 2192967−2192971 contain the supplementary crystallographic data for this paper. These data can be obtained free of charge via www.ccdc.cam.ac.uk/data_request/cif, or by emailing data_request@ccdc.cam.ac.uk, or by contacting The Cambridge Crystallographic Data Centre, 12 Union Road, Cambridge CB2 1EZ, UK; fax: +44 1223 336033.

■ AUTHOR INFORMATION

Corresponding Author

Michael J. Ingleson − *School of Chemistry, University of Edinburgh, Edinburgh EH9 3FJ, U.K.*; orcid.org/0000-0001-9975-8302; Email: michael.ingleson@ed.ac.uk

Authors

Clément R. P. Millet − *School of Chemistry, University of Edinburgh, Edinburgh EH9 3FJ, U.K.*

Jürgen Pahl − *School of Chemistry, University of Edinburgh, Edinburgh EH9 3FJ, U.K.*

Emily Noone − *School of Chemistry, University of Edinburgh, Edinburgh EH9 3FJ, U.K.*

Kang Yuan − *School of Chemistry, University of Edinburgh, Edinburgh EH9 3FJ, U.K.*

Gary S. Nichol − *School of Chemistry, University of Edinburgh, Edinburgh EH9 3FJ, U.K.*

Marina Uzelac − *School of Chemistry, University of Edinburgh, Edinburgh EH9 3FJ, U.K.*

Complete contact information is available at: https://pubs.acs.org/10.1021/acs.organomet.2c00393

Author Contributions

The manuscript was written through contributions of all authors. All authors have given approval to the final version of the manuscript.

Notes

The authors declare no competing financial interest.

■ ACKNOWLEDGMENTS

This project has received funding from the European Research Council (ERC) under the European Union's Horizon 2020 research and innovation programme (grant agreement no.

769599). We thank the mass spectrometry facility (SIRCAMS) at the University of Edinburgh for carrying out MS analysis.

REFERENCES

(1) For reviews see: (a) Neeve, E. C.; Geier, S. J.; Mkhalid, I. A. I.; Westcott, S. A.; Marder, T. B. Diboron(4) Compounds: From Structural Curiosity to Synthetic Workhorse. *Chem. Rev.* **2016**, *116*, 9091−9161. (b) Cuenca, A. B.; Shishido, R.; Ito, H.; Fernández, E. Transition-metal-free B−B and B−interelement reactions with organic molecules. *Chem. Soc. Rev.* **2017**, *46*, 415.

(2) (a) Finch, A.; Schlesinger, H. I. Diboron Tetrafluoride. *J. Am. Chem. Soc.* **1958**, *80*, 3573−3574. For a review see: (b) Morrison, J. A. Chemistry of the Polyhedral Boron Halides and the Diboron Tetrahalides. *Chem. Rev.* **1991**, *91*, 35−48.

(3) For a recent review see: (a) Légaré, M. A.; Pranckevicius, C.; Braunschweig, H. Metallomimetic Chemistry of Boron. *Chem. Rev.* **2019**, *119*, 8231−8261. For select work since this review see: (b) Schmidt, U.; Werner, L.; Arrowsmith, M.; Deissenberger, A.; Hermann, A.; Hofmann, A.; Ullrich, S.; Mattock, J. D.; Vargas, A.; Braunschweig, H. trans-Selective Insertional Dihydroboration of a cis-Diborene: Synthesis of Linear sp^3 -sp^2 -sp^3 -Triboranes and Subsequent Cationization. *Angew. Chem., Int. Ed.* **2020**, *59*, 325−329. (c) Schön, F.; Greb, L.; Kaifer, E.; Himmel, H. J. Desymmetrization of Dicationic Diboranes by Isomerization Catalyzed by a Nucleophile. *Angew. Chem., Int. Ed.* **2020**, *59*, 9127−9133. (d) Bamford, K. L.; Qu, Z. W.; Stephan, D. W. Reactions of $B_2(o\text{-tolyl})_4$ with Boranes: Assembly of the Pentaborane(9), $HB[B(o\text{-tolyl})(\mu\text{-H})]_4$. *Angew. Chem., Int. Ed.* **2021**, *60*, 8532−8536. (e) Wu, L.; Kojima, C.; Lee, K. H.; Morisako, S.; Lin, Z.; Yamashita, M. Mechanistic study on the reaction of pinB-$BMes_2$ with alkynes based on experimental investigation and DFT calculations: gradual change of mechanism depending on the substituent. *Chem. Sci.* **2021**, *12*, 9806.

(4) For a review see: (a) Prey, S. E.; Wagner, M. Threat to the Throne: Can Two Cooperating Boron Atoms Rival Transition Metals in Chemical Bond Activation and Catalysis? *Adv. Synth. Catal.* **2021**, *363*, 2290−2309. For selected examples see: (b) Zhao, X.; Stephan, D. W. Bis-boranes in the frustrated Lewis pair activation of carbon dioxide. *Chem. Commun.* **2011**, *47*, 1833−1835. (c) Liu, Y. L.; Kehr, C. G.; Daniliuc, G.; Erker, G. Geminal bis-borane formation by borane Lewis acid induced cyclopropyl rearrangement and its frustrated Lewis pair reaction with carbon dioxide. *Chem. Sci.* **2017**, *8*, 1097. (d) von Grotthuss, E.; Prey, S. E.; Bolte, M.; Lerner, H. W.; Wagner, M. Dual Role of Doubly Reduced Arylboranes as Dihydrogen- and Hydride-Transfer Catalysts. *J. Am. Chem. Soc.* **2019**, *141*, 6082−6091.

(5) Wade, C. R.; Broomsgrove, A. E. J.; Aldridge, S.; Gabbaï, F. P. Fluoride Ion Complexation and Sensing Using Organoboron Compounds. *Chem. Rev.* **2010**, *110*, 3958−3984.

(6) It should be noted that bis-boranes have been used as catalysts in C-H borylation: (a) Liu, Y. L.; Kehr, G.; Daniliuc, C. G.; Erker, G. Metal-Free Arene and Heteroarene Borylation Catalyzed by Strongly Electrophilic Bis-boranes. *Chem.—Eur. J.* **2017**, *23*, 12141−12144. ; and effect borylations where one borane is nucleophilic and one electrophilic: (b) Su, Y.; Huan Do, D. C. H.; Li, Y.; Kinjo, R. Metal-Free Selective Borylation of Arenes by a Diazadiborinine via C-H/C-F Bond Activation and Dearomatization. *J. Am. Chem. Soc.* **2019**, *141*, 13729−13733.

(7) For an early example: (a) Sgro, M. J.; Dömer, J.; Stephan, D. W. Stoichiometric CO_2 reductions using a bis-borane-based frustrated Lewis pair. *Chem. Commun.* **2012**, *48*, 7253−7255. For a review see: (b) Schweighauser, L.; Wegner, H. A. Bis-Boron Compounds in Catalysis: Bidentate and Bifunctional Activation. *Chem.—Eur. J.* **2016**, *22*, 14094−14103.

(8) John, A.; Bolte, M.; Lerner, H. W.; Wagner, M. A Vicinal Electrophilic Diborylation Reaction Furnishes Doubly Boron-Doped Polycyclic Aromatic Hydrocarbons. *Angew. Chem., Int. Ed.* **2017**, *56*, 5588−5592.

(9) Pahl, J.; Noone, E.; Uzelac, M.; Yuan, K.; Ingleson, M. Borylation Directed Borylation of Indoles Using Pyrazabole Electrophiles: A One-Pot Route to C7-Borylated-Indolines. *Angew. Chem., Int. Ed.* **2022**, *61*, No. e202206230.

(10) Kobayashi, A.; Suzuki, A.; Kitamura, R. Y. M.; Yamashita, M. Formation of BCBH/BCBCl Four-Membered Rings by Complexation of Boron- and Nitrogen-Substituted Acetylene with Hydro-/Chloroboranes. *Organometallics* **2020**, *39*, 383−387.

(11) (a) Hergel, A.; Pritzkow, H.; Siebert, W. Synthesis and Reactivity of a Naphtho[1,8-*bc*] boret. *Angew. Chem., Int. Ed.* **1994**, *33*, 1247−1248. (b) Kitamura, R.; Suzuki, K.; Yamashita, M. Dimerization of boryl- and amino-substituted acetylenes by B_2C_2 four-membered ring formation. *Chem. Commun.* **2018**, *54*, 5819.

(12) (a) Banister, A. J.; Greenwood, N. N.; Straughan, B. P.; Walker, J. 193. Monomeric dimethylaminoboron dihalides. *J. Chem. Soc.* **1964**, 995−1000. (b) Nöth, H.; Vahrenkamp, H. Investigations of boron compounds by nuclear magnetic resonance, II. Monomer-dimer equilibria in aminoboranes. *Chem. Ber.* **1967**, *100*, 3353−3362.

(13) Jaska, C. A.; Temple, K.; Lough, A. J.; Manners, I. Transition Metal-Catalyzed Formation of Boron−Nitrogen Bonds: Catalytic Dehydrocoupling of Amine-Borane Adducts to Form Aminoboranes and Borazines. *J. Am. Chem. Soc.* **2003**, *125*, 9424−9434.

(14) (a) Clark, E. R.; Del Grosso, A.; Ingleson, M. J. The Hydride-Ion Affinity of Borenium Cations and Their Propensity to Activate H_2 in Frustrated Lewis Pairs. *Chem.—Eur. J.* **2013**, *19*, 2462−2466. For a recent review on borenium cations see: (b) Tan, X.; Wang, H. *Chem. Soc. Rev.* **2022**, *51*, 2583.

(15) Del Grosso, A.; Ayuso Carrillo, J.; Ingleson, M. J. Regioselective electrophilic borylation of haloarenes. *Chem. Commun.* **2015**, *51*, 2878−2881.

(16) McLellan, R.; Kennedy, A. R.; Orr, S. A.; Robertson, S. D.; Mulvey, R. E. Lithium Dihydropyridine Dehydrogenation Catalysis: A Group 1 Approach to the Cyclization of Diamine Boranes. *Angew. Chem., Int. Ed.* **2017**, *56*, 1036−1041.

(17) (a) Devillard, M.; Brousses, R.; Miqueu, K.; Bouhadir, G.; Bourissou, D. A Stable but Highly Reactive Phosphine-Coordinated Borenium: Metal-free Dihydrogen Activation and Alkyne 1,2-Carboboration. *Angew. Chem., Int. Ed.* **2015**, *54*, 5722−5726. (b) Devillard, M.; Mallet-Ladeira, S.; Bouhadir, G.; Bourissou, D. Diverse reactivity of borenium cations with >N-H compounds. *Chem. Commun.* **2016**, *52*, 8877. (c) Saida, A. B.; Chardon, A.; Osi, A.; Tumanov, N.; Wouters, J.; Adjieufack, A. I.; Champagne, B.; Berionni, G. Pushing the Lewis Acidity Boundaries of Boron Compounds With Non-Planar Triarylboranes Derived from Triptycenes. *Angew. Chem., Int. Ed.* **2019**, *58*, 16889−16893. (d) Osi, A.; Mahaut, D.; Tumanov, N.; Fusaro, L.; Wouters, J.; Champagne, B.; Chardon, A.; Berionni, G. Taming the Lewis Superacidity of Non-Planar Boranes: C-H Bond Activation and Non-Classical Binding Modes at Boron. *Angew. Chem., Int. Ed.* **2022**, *61*, No. e202112342.

(18) (a) Clay, J. M.; Vedejs, E. Hydroboration with Pyridine Borane at Room Temperature. *J. Am. Chem. Soc.* **2005**, *127*, 5766−5767. (b) Prokofjevs, A.; Boussonnière, A.; Li, L.; Bonin, H.; Lacôte, E.; Curran, D. P.; Vedejs, E. Borenium Ion Catalyzed Hydroboration of Alkenes with N-Heterocyclic Carbene-Boranes. *J. Am. Chem. Soc.* **2012**, *134*, 12281−12288. (c) McGough, J. S.; Cid, J.; Ingleson, M. J. Catalytic Electrophilic C−H Borylation Using NHC·Boranes and Iodine Forms C2-, not C3-, Borylated Indoles. *Chem.—Eur. J.* **2017**, *23*, 8180−8184.

(19) Prokofjevs, A.; Jermaks, J.; Borovika, A.; Kampf, J. W.; Vedejs, E. Electrophilic C-H Borylation and Related Reactions of B-H Boron cations. *Organometallics* **2013**, *32*, 6701−6711.

(20) Krossing, I.; Raabe, I. Noncoordinating Anions-Fact or Fiction? A Survey of Likely Candidates. *Angew. Chem., Int. Ed.* **2004**, *43*, 2066−2090.

(21) Ciobanu, O.; Kaifer, E.; Enders, M.; Himmel, H. J. Synthesis of a Stable $B_2H_5^+$ Analogue by Protonation of a Double Base-Stabilized Diborane(4). *Angew. Chem., Int. Ed.* **2009**, *48*, 5538−5541.

(22) Nie, Y.; Pritzkow, H.; Siebert, W. Synthesis and Structure of Pyrrolidinobromodiboranes(4). *Z. Naturforsch.* **2005**, *60*, 1016−1019.

https://doi.org/10.1021/acs.organomet.2c00393
Organometallics XXXX, XXX, XXX−XXX

(23) (a) Metzler, N.; Nöth, H. A Deceiving X-ray Single-Crystal Structure Determination: Amino-Hydrogen Exchange in Amino-alkynylboranes and ab initio Investigations of Alkynylboranes, Borirenes, and Boraallenes. *Chem. Ber.* **1995**, *128*, 711−717. (b) Maringgele, W.; Noltemeyer, M.; Schmidt, HG.; Meiler, A. Sterically Encumbered Monomeric Sec.amino-(halogeno)-hydroboranes and the Corresponding Dihalogeno- and Dihydroborane Precursors. *Main Group Met. Chem.* **1999**, *22*, 715−732.
(24) (a) Solovyev, A.; Chu, Q.; Geib, S. J.; Fensterbank, L.; Malacria, M.; Lacôte, E.; Curran, D. P. Substitution Reactions at Tetracoordinate Boron: Synthesis of N-Heterocyclic Carbene Boranes with Boron−Heteroatom Bonds. *J. Am. Chem. Soc.* **2010**, *132*, 15072−15080. (b) Muessig, J. H.; Thaler, M.; Dewhurst, R. D.; Paprocki, V.; Seufert, J.; Mattock, J. D.; Vargas, A.; Braunschweig, H. Phosphine-Stabilized Diiododiborenes: Isolable Diborenes with Six Labile Bonds. *Angew. Chem., Int. Ed.* **2019**, *58*, 4405−4409. (c) Kundu, G.; Ajithkumar, V. S.; Raj, K. V.; Vanka, K.; Tothadi, S.; Sen, S. S. Substitution at sp^3 boron of a six-membered NHC-BH_3: convenient access to a dihydroxyborenium cation. *Chem. Commun.* **2022**, *58*, 3783.
(25) (a) Škoch, K.; Chen, C.; Daniliuc, C. G.; Kehr, G.; Erker, G. A deprotonation pathway to reactive [B]=CH_2 boraalkenes. *Dalton Trans.* **2022**, *51*, 7695−7704. (b) Morgan, M.; Patrick, E. A.; Rautiainen, J. M.; Tuononen, H. M. W. E.; Piers, D. M.; Spasyuk, D. M. Zirconocene-Based Methods for the Preparation of BN-Indenes: Application to the Synthesis of 1,5-Dibora-4a,8a-diaza-1,2,3,5,6,7-hexaaryl-4,8-dimethyl-s-indacenes. *Organometallics* **2017**, *36*, 2541−2551.
(26) (a) Ziegler, M. L.; Weidenhammer, K.; Autenrieth, K.; Friebolin, H. Die Molekül- und Kristallstrukturen von Methyl(4-Br-phenyl)amino-chlorphenylboran, $(BrC_6H_4)(CH_3)NB(Cl)(C_6H_5)$, und Methyl(2-methyl-4-Br-plienyl)amino-clilor(2-metliylphenyl)-boran, $(BrC_7H_6)(CH_3)NB(Cl)(C_7H_7)$. *Z. Naturforsch.* **1978**, *33*, 200−208. (b) Wojnowski, W.; Przyjemska, K.; Peters, K.; von Schnering, H. G.; von Bennigsen-Mackiewicz, T.; Paetzold, P. Darstellung und Struktur von tert-Butyl(tert-butylamino)-[tris(tert-butyloxy)silylthio]boran. *Z. Anorg. Allg. Chem.* **1988**, *556*, 92−96. (c) Braunschweig, H.; von Koblinski, C.; Mamuti, M.; Englert, U.; Wang, R. Synthesis and Structure of [1]Borametallocenophanes of Titanium, Zirconium, and Hafnium. *Eur. J. Inorg. Chem.* **1999**, *1999*, 1899−1904. (d) Braunschweig, H.; Kraft, M.; Radacki, K.; Stellwag, S. Piperidino Substituted [1]Borametallocenophanes. Synthesis, Reactivity, and Structure. *Z. Naturforsch.* **2006**, *61*, 509−516. (e) Braunschweig, H.; Ewing, W. C.; Geetharani, K.; Schäfer, M. The Reactivities of Iminoboranes with Carbenes: BN Isosteres of Carbene-Alkyne Adducts. *Angew. Chem., Int. Ed.* **2015**, *54*, 1662−1665.
(27) Burford, R. J.; Geier, M. J.; Vogels, C. M.; Decken, A.; Westcott, S. A. Addition of boranes to iminophosphines: Synthesis and reactivity of a new bulky hydroboration reagent. *J. Organomet. Chem.* **2013**, *731*, 1−9.
(28) Trefonas, L. M.; Mathews, F. S.; Lipscomb, W. N. The Molecular and Crystal Structure of $(BH_2)_3[N(CH_3)_2]_3$. *Acta Crystallogr.* **1961**, *14*, 273−278.
(29) For a recent paper covering this topic in depth see: Jayaraman, A.; Powell-Davies, H.; Fontaine, F.-G. Revisiting the reduction of indoles by hydroboranes: A combined experimental and computational study. *Tetrahedron* **2019**, *75*, 2118−2127.
(30) Chavant, P. Y.; Vaultier, M. Preparation of some organo-bis(diisopropylamino)boranes and their application to the synthesis of oxazaborolidines. *J. Organomet. Chem.* **1993**, *455*, 37−46.
(31) (a) Lindenau, K.; Jannsen, N.; Rippke, M.; Al Hamwi, H. A.; Selle, C.; Drexler, H. J.; Spannenberg, A.; Sawall, M.; Neymeyr, K.; Heller, D.; Reiß, F.; Beweries, T. Mechanistic insights into dehydrocoupling of amine boranes using dinuclear zirconocene complexes. *Catal. Sci. Technol.* **2021**, *11*, 4034−4050. (b) Brodie, C. N.; Boyd, T. M.; Sotorríos, L.; Ryan, D. E.; Magee, E.; Huband, S.; Town, J. S.; Lloyd-Jones, G. C.; Haddleton, D. M.; Macgregor, S. A.; Weller, A. S. Controlled Synthesis of Well-Defined Polyaminoboranes on Scale Using a Robust and Efficient Catalyst. *J. Am. Chem. Soc.* **2021**, *143*, 21010−21023.
(32) Yuan, K.; Volland, D.; Kirschner, S. M. G. S. A.; Uzelac, M. J.; Nichol, G. S.; Nowak-Król, A.; Ingleson, M. J. Enhanced N-directed electrophilic C-H borylation generates BN-[5]- and [6]helicenes with improved photophysical properties. *Chem. Sci.* **2022**, *13*, 1136−1145.
(33) Ihara, E.; Young, V. G., Jr.; Jordan, R. F. Cationic Aluminum Alkyl Complexes Incorporating Aminotroponiminate Ligands. *J. Am. Chem. Soc.* **1998**, *120*, 8277−8278.
(34) Orr, S. A.; Kennedy, A. R.; Liggat, J. J.; McLellan, R.; Mulvey, R. E.; Robertson, S. D. Accessible heavier s-block dihydropyridines: structural elucidation and reactivity of isolable molecular hydride sources. *Dalton Trans.* **2016**, *45*, 6234−6240.
(35) (a) Vance, J. R.; Robertson, A. P. M.; Lee, K.; Manners, I. Photoactivated, Iron-Catalyzed Dehydrocoupling of Amine-Borane Adducts: Formation of Boron-Nitrogen Oligomers and Polymers. *Chem.—Eur. J.* **2011**, *17*, 4099−4103. (b) Vance, J. R.; Schäfer, A.; Robertson, A. P. M.; Lee, K.; Turner, J.; Whittell, G. R.; Manners, I. Iron-Catalyzed Dehydrocoupling/Dehydrogenation of Amine-Boranes. *J. Am. Chem. Soc.* **2014**, *136*, 3048−3064.
(36) Jaska, C. A.; Temple, K.; Lough, A. J.; Manners, I. Rhodium-catalyzed formation of boron-nitrogen bonds: A mild route to cyclic aminoboranes and borazines. *Chem. Commun.* **2001**, *11*, 962−963.

https://doi.org/10.1021/acs.organomet.2c00393
Organometallics XXXX, XXX, XXX−XXX